



An Analytical Solution of Wave Motion in a Transversely Isotropic Poroelastic Half-Space Underlying a Liquid Layer

Teymouri, H.¹, Khojasteh, A.^{2*}, Rahimian, M.³ and Pak, R.Y.S.⁴

¹ Ph.D. Candidate, School of Civil Engineering, College of Engineering, University of Tehran, Tehran, Iran.

² Assistant Professor, College of Engineering, University of Tehran, Tehran, Iran.

³ Professor, School of Civil Engineering, College of Engineering, University of Tehran, Tehran, Iran.

⁴ Professor, College of Engineering and Applied Science, University of Colorado Boulder, Boulder, USA.

© University of Tehran 2021

Received: 23 Jun. 2019;

Revised: 23 Dec. 2019;

Accepted: 03 Feb. 2020

ABSTRACT: In this paper, an analytical method is developed for the axisymmetric dynamic response of a finite thickness liquid layer overlying a transversely isotropic porous solid half-space due to body waves. Potential functions and integral transforms are used together to handle the equations of wave motion in two media. The time-harmonic excitation with axisymmetric shape is assumed to be distributed in the interface of liquid and porous media. Green's functions of stress and displacement are derived as closed-form integral expressions. Demonstration of the effect of the liquid thickness, degree of material anisotropy, and frequency of excitation on the dynamic response is considered here. Numerical results for a uniform distributed disk load are comprised with the existing elastic and poroelastic solutions to illustrate the quality of the method. The results of the current paper can be used in analysis and modelling the rigid or flexible foundations in marine structures.

Keywords: Green's Functions, Poroelastodynamics, Potential Functions, Wave Motion.

1. Introduction

Body waves in earth's layers can be produced by many phenomena like landslide, submarine earthquakes, foundations with dynamic loads and etc. Study of wave motion in different media is an important subject due to their applications in geophysics, earthquake engineering and similar fields. In many researches, the medium of the earth surfaced is modeled as a semi-infinite half-

space. Many of studies on elastodynamic problems are based on the consideration of the half-space as a single phase solid. However, in real problems in geophysics and earthquake engineering, the half-space is consisting of two-phased poroelastic continuum. The dynamic response of fluid-saturated porous media is of interest in geophysics, acoustic, and soil mechanics. The first theory of wave motion in such media has been developed since Biot's work on fluid saturated materials (Biot,

* Corresponding author E-mail: akhojasteh@ut.ac.ir

1956a,b). Also poroelastic formulation has been extended for anisotropic materials (Cheng, 1997). Equations of motion for time-harmonic excitation in poroelastodynamics have been formulated (Senjuntichai and Rajapakse, 1994). Wave equations in saturated porous media have been considered and the response of such media under time-harmonic plane waves is evaluated (Sharma and Gogna, 1991; Sharma, 2008). In many researches porous media has been assumed as isotropic material. However, in reality because of the original deposition or microstructural characteristic, these media have transversely isotropic behavior.

Potential functions are used in wide range in elastodynamic problems. When the Helmholtz decomposition method is the approach to solve the equations, use of these functions is the best way. In the study of transversely isotropic half-space, an efficient method is presented to determine the displacement and stress fields (Raofian Naeeni and Eskandari-Ghadi, 2014). Scalar potential functions have an important role in solving the wave equations of transversely isotropic materials (Eskandari-Ghadi, 2005).

Surface waves in models which were consist of a liquid layer, overlying on the transversely isotropic solid mediums is an interesting issue in marine studies (Bagheri et al., 2016). By using the scalar potential functions, the Greens functions of poroelastic medium have been introduced (Pooladi et al., 2017; Sahebkar and Eskandari-Ghadi, 2016). In another study reflection of plane waves at boundaries of a liquid filled poroelastic half-space was established (Tajuddin and Hussaini, 2005). The wave propagation in the porous medium is considered in many studies by different methods (Keawsawasvong and Senjuntichai, 2019). Also for an isotropic poroelastic seabed, some studies have been done to determine the effect of the properties of the medium on the behavior of the structure or the considered medium (Keawsawasvong and Senjuntichai, 2018;

Feng et al., 2016; Yamamoto, 2008; Teymouri et al., 2019).

In this paper, the Green's functions of displacement and stress fields of two-layered media, consist of a liquid layer with finite thickness and a poroelastic half-space, are determined. Integral transforms and potential functions are used to solve the equations of motion of subdomains. The load is assumed with axisymmetric shape in an arbitrary depth at the liquid layer. To verify results, comparisons with the existing researches are exhibited.

The interaction between the rigid or flexible foundations and soil is an interesting subject in the civil engineering. Many studies have been established to determine the behavior of a disc in the soil medium (Ahmadi and Eskandari, 2014). To solve the equations of such problems in an analytical way, the Green's functions are needed and the results of the present study can be applied directly in the formulation of the foundations or pile problems in the marine medium. A liquid layer which is overlying a porous layer is commonly encountered in offshore and marine structures (Lian-Zhou et al., 2017). Foundation and piles under seas or oceans are the most practical problems of such mediums. Reservoirs of dams are other similar examples of this configuration. So the results and analytical procedure of current study can be applied to achieve dynamic response of such media. By considering the effect of pore pressure effect on the marine structures, the analysis introduced here can be applied in the dynamic analysis of such structures, especially for the flexible or rigid foundations.

2. Statement of the Problem and Governing Equations

Figure 1, shows the geometry of the problem. The origin of the coordinates is located on the free surface of the liquid layer. A liquid with the depth of h , is overlying on a poroelastic half space. The

time-harmonic exciting load is located in the depth of s , in liquid layer.

2.1. Governing Equations

The equations of motion in u - p formulation, which consists of displacements of solid skeleton and pore fluid pressure as the unknowns, for a transversely isotropic poroelastic medium, in the absence of body forces, subjected to a time-harmonic excitation can be represented as (Pooladi et al. 2017):

$$\begin{aligned}
 & A_{66} \left(\nabla_{r\theta}^2 u_r^p - \frac{1}{r^2} u_r^p \right) + (A_{66} + A_{12}) \frac{\partial e}{\partial r} + \\
 & A_{44} \frac{\partial^2 u_r^p}{\partial z^2} + (A_{44} + A_{13}) \frac{\partial^2 u_z^p}{\partial r \partial z} + \\
 & \rho_{r\theta}^c \omega^2 u_r^p + \alpha_{r\theta}^c \frac{\partial p^p}{\partial r} = 0; \\
 & A_{66} \nabla_{r\theta}^2 u_z^p + (A_{44} + A_{13}) \frac{\partial e}{\partial z} \\
 & + A_{33} \frac{\partial^2 u_z^p}{\partial z^2} + \rho_z^c \omega^2 u_z^p \\
 & + \alpha_z^c \frac{\partial p^p}{\partial z} = 0; \\
 & \left(\alpha_{r\theta}^c e + \frac{K_{r\theta}}{(i\omega)} \nabla_{r\theta}^2 p^p \right) + \\
 & \left(\alpha_z^c \frac{\partial u_z^p}{\partial z} + \frac{K_z}{(i\omega)} \frac{\partial^2 p^p}{\partial z^2} \right) - \frac{p^p}{M} = 0;
 \end{aligned} \tag{1}$$

where:

$$\begin{aligned}
 e &= \frac{\partial u_r^p}{\partial r} + \frac{u_r^p}{r} \\
 \nabla_{r\theta}^2 &= \frac{\partial^2}{\partial r^2} + \frac{1}{r} \frac{\partial}{\partial r} \\
 K_i(\omega) &= \left(\frac{1}{(i\omega)m_i + b_i} \right) \\
 \rho_i^c &= \left(\rho + \rho_f \omega^2 \frac{K_i}{(i\omega)} \right) \\
 \alpha_i^c &= - \left(\beta_i + \rho_f \omega^2 \frac{K_i}{(i\omega)} \right) \\
 (i &= z, r\theta)
 \end{aligned} \tag{2}$$

in which A_{ij} : are elasticity constants of solid skeleton, u_i^p ($i = r, z$): represent the time-harmonic displacements of solid

skeleton, p^p : denotes the pore fluid pressure,

$$\begin{aligned}
 m_i &= T_i \rho_f / \phi \\
 b_i &= F_i \eta / \kappa_i \quad (i = z, r\theta)
 \end{aligned} \tag{3}$$

are the corresponding viscous and inertial coupling parameters respectively. η , κ_i and T_i : represent the viscosity of the pore fluid, the intrinsic permeability and the tortuosity of the porous medium, respectively. Also ϕ : is the porosity of the medium and F_i : is the viscosity correction factor and has the value of:

$$F_i = \sqrt{1 + i\alpha_g \frac{\omega}{\omega_{ci}}} \tag{4}$$

where β_i ($i = z, r\theta$) and $M = 1/\beta$: denote Biot's Skeletal and pore fluid compressibility parameters. ω , ρ and ρ_f : represent the frequency, and densities of solid skeleton and pore fluid respectively. $\omega_{ci} = \eta / m_i \kappa_i$: denotes the characteristic frequencies for the material symmetry axis, z and over the plane of material symmetry, $r\theta$. α_g : is the pore geometry shape factor.

Also K , ρ^c and α^c : define the complex permeability coefficients, mass densities and Biot's effective stress coefficients.

It should be noted that all the above equations are based on Darcy's law and are useful only to laminar flow between the solid and pore structures. In order to uncouple the equations, a method of potential functions is employed. The function F is assumed as a scalar potential function, which displacement and pressure fields can be expressed as:

$$\begin{aligned}
 u_r^p &= \frac{\partial^2}{\partial r \partial z} \Delta_{r\theta} F, \\
 u_z^p &= \Delta_z F, \\
 p^p &= \Delta_p \frac{\partial}{\partial z} F
 \end{aligned} \tag{5}$$

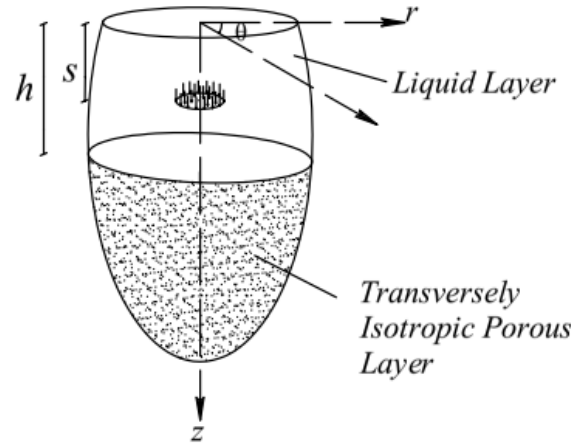


Fig. 1. Geometry of the system

where:

$$\begin{aligned}\Delta_{r\theta} &= -(\bar{K}_{r\theta}\alpha_3\Delta_p - (i\omega)\bar{\alpha}_{r\theta}\bar{\alpha}_z) \\ \Delta_z &= (\bar{K}_{r\theta}(1+\alpha_1)\Delta_\alpha\Delta_p - (i\omega)\bar{\alpha}_{r\theta}^2\nabla_{r\theta}^2) \\ \Delta_p &= -(i\omega)\left((1+\alpha_1)\bar{\alpha}_z\nabla_\alpha - \alpha_3\bar{\alpha}_{r\theta}\nabla_{r\theta}^2\right) \\ \nabla_\alpha &= \nabla_{r\theta}^2 + \frac{\alpha_2}{(1+\alpha_1)}\frac{\partial^2}{\partial z^2} + \frac{\bar{\rho}_{r\theta}}{(1+\alpha_1)}\omega^2 \\ \nabla_p &= \nabla_{r\theta}^2 + \frac{\bar{K}_z}{\bar{K}_{r\theta}}\frac{\partial^2}{\partial z^2} - \frac{\bar{\beta}}{\bar{K}_{r\theta}}(i\omega)\end{aligned}\quad (6)$$

and

$$\begin{aligned}\alpha_1 &= \frac{A_{66} + A_{12}}{A_{66}} \\ \bar{K}_i &= \frac{K_i}{A_{66}} \\ \alpha_2 &= \frac{A_{44}}{A_{66}} \\ \bar{\rho}_i &= \frac{\rho_i^c}{A_{66}} \\ \alpha_3 &= \frac{A_{13} + A_{44}}{A_{66}} \\ \bar{\alpha}_i &= \frac{\alpha_i^c}{A_{66}} \quad (i = z, r\theta)\end{aligned}\quad (7)$$

Substitution of Eq. (3), in Eq. (1), gives the partial differential equation in terms of F as:

$$\left(\alpha_2\nabla_\beta\Delta_z + \alpha_3\frac{\partial^2}{\partial z^2}\nabla_{r\theta}^2\Delta_{r\theta} + \bar{\alpha}_z\frac{\partial^2}{\partial z^2}\Delta_p\right)F = 0$$

Hankel transform of Eq. (7), is as:

$$\left(\alpha_2\bar{\nabla}_\beta^m\bar{\Delta}_z^m + \alpha_3\bar{\nabla}_{r\theta}^{m^2}\bar{\nabla}_{r\theta}^m\frac{d^2}{dz^2} + \bar{\alpha}_z\bar{\Delta}_p^m\frac{d^2}{dz^2}\right)F^m = 0\quad (8)$$

where

$$\begin{aligned}\bar{\Delta}_{r\theta}^m &= -(\bar{K}_{r\theta}\alpha_3\bar{\nabla}_p^m - (i\omega)\bar{\alpha}_{r\theta}\bar{\alpha}_z) \\ \Delta_z^m &= (\bar{K}_{r\theta}(1+\alpha_1)\bar{\nabla}_\alpha^m\bar{\nabla}_p^m - (i\omega)\bar{\alpha}_{r\theta}^2\bar{\nabla}_{r\theta}^{m^2}) \\ \bar{\Delta}_p^m &= -(i\omega)\left((1+\alpha_1)\bar{\alpha}_z\bar{\nabla}_\alpha^m - \alpha_3\bar{\alpha}_{r\theta}\bar{\nabla}_{r\theta}^{m^2}\right) \\ \bar{\nabla}_p^m &= -\xi^2 + \frac{\bar{K}_z}{\bar{K}_{r\theta}}\frac{d^2}{dz^2} - \frac{\bar{\beta}}{\bar{K}_{r\theta}}(i\omega) \\ \bar{\nabla}_\alpha^m &= -\xi^2 + \frac{\alpha_2}{(1+\alpha_1)}\frac{d^2}{dz^2} + \frac{\bar{\rho}_{r\theta}}{(1+\alpha_1)}\omega^2 \\ \bar{\nabla}_\beta^m &= -\xi^2 + \frac{\alpha_4}{\alpha_2}\frac{d^2}{dz^2} + \frac{\bar{\rho}_z}{\alpha_2}\omega^2 \\ \bar{\nabla}_0^m &= -\xi^2 + \alpha_2\frac{d^2}{dz^2} + \bar{\rho}_{r\theta}\omega^2 \\ \bar{\nabla}_{r\theta}^{m^2} &= -\xi^2\end{aligned}\quad (10)$$

In the above equations m : denotes the order of Hankel transform. Eq. (8) can be represented as:

$$\left(\frac{d^6}{dz^6} + a_1\frac{d^4}{dz^4} + a_2\frac{d^2}{dz^2} + a_3\right)F^m = 0\quad (11)$$

where:

$$\begin{aligned}
 a_1 &= C_p + \left(C_\alpha + C_\beta + \frac{\alpha_3^2}{\alpha_2 \alpha_4} \xi^2 \right) - \frac{(i\omega) \bar{\alpha}_z^2}{\bar{K}_z \alpha_4}; \\
 a_2 &= C_\alpha C_\beta + C_p \left(C_\alpha + C_\beta + \frac{\alpha_3^2}{\alpha_2 \alpha_4} \xi^2 \right) + \\
 &\left(C_m \xi^2 - \frac{\bar{\rho}_{r\theta}}{\alpha_2} \omega^2 \right) \frac{(i\omega) \bar{\alpha}_z^2}{\bar{K}_z \alpha_4}; \\
 a_3 &= C_\beta \left(C_\alpha C_p + \frac{(i\omega) \bar{\alpha}_{r\theta}^2}{\bar{K}_z} \xi^2 \right); \\
 C_\alpha &= \frac{(1 + \alpha_1)}{\alpha_2} \left(\frac{\bar{\rho}_{r\theta}}{(1 + \alpha_1)} \omega^2 - \xi^2 \right); \\
 C_\beta &= \frac{\alpha_2}{\alpha_4} \left(\frac{\bar{\rho}_z}{\alpha_2} \omega^2 - \xi^2 \right); \\
 C_p &= -\frac{\bar{K}_{r\theta}}{\bar{K}_z} \left(\frac{(i\omega) \bar{\beta}}{\bar{K}_{r\theta}} + \xi^2 \right); \\
 C_m &= \frac{\alpha_4 \bar{\alpha}_{r\theta}^2 - 2\alpha_3 \bar{\alpha}_{r\theta} \bar{\alpha}_z + \bar{\alpha}_z^2 (1 + \alpha_1)}{\alpha_2 \bar{\alpha}_z^2};
 \end{aligned} \tag{12}$$

Eq. (11) is a differential equation of sixth order based on the terms of potential function and it has a general solution as:

$$\begin{aligned}
 F_m^m(\xi, z) &= A_m(\xi) e^{-\lambda_1 z} + \\
 B_m(\xi) e^{-\lambda_2 z} &+ C_m(\xi) e^{-\lambda_3 z}
 \end{aligned} \tag{13}$$

where A_m , B_m and C_m : are the unknown functions of ξ , that will be calculated from appropriate boundary conditions. Because of radiation condition in half-space, the answers with positive λ are neglected. In the above solution λ_i can be achieved by getting $\alpha_3 = 0$ and are multi-valued functions. To make these functions as single-valued branch cuts that emanate from ξ_i are

specified (the roots of λ_i) as Figure 2.

$$\begin{aligned}
 \lambda_i &= \sqrt{-\frac{1}{3} \left(a_1 + \delta_i D + \frac{\Delta_0}{\delta_i D} \right)} \\
 (i &= 1, 2, 3)
 \end{aligned} \tag{14}$$

where

$$\begin{aligned}
 \Delta_0 &= (a_1^2 - 3a_2) \\
 \delta_1 &= 1 \\
 \Delta_1 &= (2a_1^3 - 9a_1 a_2 + 27a_3) \\
 \delta_2 &= \left(\frac{-1 + \sqrt{3}i}{2} \right) \\
 D &= \sqrt[3]{\frac{\Delta_1 + \sqrt{\Delta_1^2 - 4\Delta_0^3}}{2}} \\
 \delta_3 &= \left(\frac{-1 - \sqrt{3}i}{2} \right)
 \end{aligned} \tag{15}$$

and

$$\begin{aligned}
 \xi_1 &= \\
 &\pm \sqrt{-\frac{(i\omega)}{2K_{r\theta}(1 + \alpha_1)} \left(s + \sqrt{s^2 - 4K_{r\theta}(1 + \alpha_1)(i\omega) \bar{\beta} \bar{\rho}_{r\theta}} \right)}; \\
 \xi_2 &= \\
 &\pm \sqrt{-\frac{(i\omega)}{2K_{r\theta}(1 + \alpha_1)} \left(s - \sqrt{s^2 - 4K_{r\theta}(1 + \alpha_1)(i\omega) \bar{\beta} \bar{\rho}_{r\theta}} \right)}; \\
 \xi_3 &= \\
 &\pm \sqrt{\frac{\bar{\rho}_z}{\alpha_2} \omega}; \\
 s &= (\bar{\beta}(1 + \alpha_1) + (i\omega)K_{r\theta} \bar{\rho}_{r\theta} + \bar{\alpha}_{r\theta}^2)
 \end{aligned} \tag{16}$$

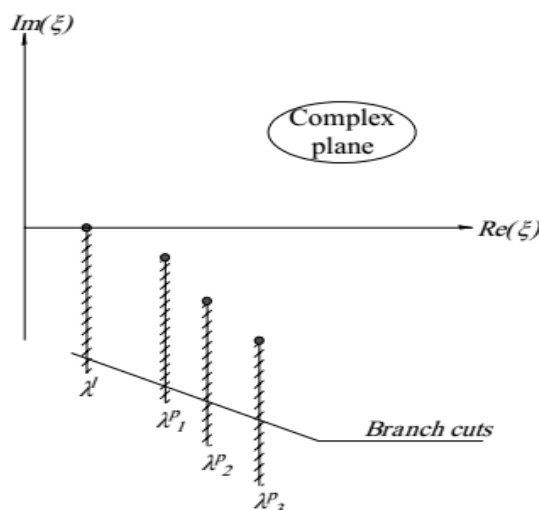


Fig. 2. Schematic position of branch cuts

Now the pressure, stress and displacement fields can be represented in Hankel transformed state of potential function as (Pooladi et al., 2017):

$$\begin{aligned} u_z^m &= \bar{\Delta}_z^m F^m; \\ p^m &= \bar{\Delta}_p^m \frac{d}{dz} F^m; \\ \sigma_{zz}^m &= A_{66}(\alpha_4 \bar{\Delta}_z^m - (\alpha_3 - \alpha_2) \xi^2 \bar{\Delta}_{r\theta}^m - \\ &\quad \bar{\beta}_z \bar{\Delta}_p^m) \frac{d}{dz} F^m; \\ \sigma_{zr}^{m+1} &= -A_{66} \alpha_2 \xi \left(\bar{\Delta}_z^m + \bar{\Delta}_{r\theta}^m \frac{d^2}{dz^2} \right) F^m; \end{aligned} \quad (17)$$

Equations of motion for liquid layer in Hankel transformed state with respect to the potential function φ can be noticed as (Bagheri et al., 2016):

$$\left(\frac{\rho_f \omega^2}{K} - \xi^2 + \frac{d^2}{dz^2} \right) \varphi = 0 \quad (18)$$

which has the general solution as:

$$\begin{aligned} \varphi(\xi, z) &= S(\xi) e^{-\lambda_4 z} + R(\xi) e^{\lambda_4 z} \\ \lambda_4 &= \sqrt{\xi^2 - \frac{\omega^2}{c_1^2}} \\ c_1 &= \sqrt{K / \rho_f} \end{aligned} \quad (19)$$

where S and R : are unknown functions of ξ , and will be calculated from Boundary Conditions. K : represents bulk module of liquid. Pressure and displacements in liquid layer can be written as:

$$\begin{aligned} u_z^l &= \frac{\partial \varphi}{\partial z} \\ \sigma_{zz}^l &= -p^l = -\rho_f \omega^2 \varphi \end{aligned} \quad (20)$$

2.2. Boundary Conditions

Liquid layer is subdivided into two layers (*Layer I*: $0 < z < s$ and *Layer II*: $s < z < h$), which layer *I* is in contact with the air (zero pressure) and layer *II* is in contact

with porous half-space.

In layer *I* at $z = 0$ pressure is equal to zero so the potential function should have the form of:

$$\varphi^I(\xi, z) = S^I \sinh(\lambda_4 z) \quad (21)$$

In contrary, in layer *II* we have:

$$\varphi^{II}(\xi, z) = S^{II} e^{-\lambda_3 z} + R^{II} e^{\lambda_3 z} \quad (22)$$

There are two sets of Boundary Conditions, one in $z = s$ (load depth) and the other is at $z = h$ (interface between liquid and half-space). At $z = s$:

$$\begin{aligned} \sigma_{zz}^l(r, s^-) - \sigma_{zz}^l(r, s^+) &= \begin{cases} R(r) & (r) \in \Pi \\ 0 & (r) \notin \Pi \end{cases} \\ u_z^l(r, s^-) - u_z^l(r, s^+) &= 0 \end{aligned} \quad (23)$$

where R : is the function of excitation and Π : is region of loading. At $z = h$ (Cheng, 2016):

$$\begin{aligned} u_z^p(r, z = h^+) + \phi \cdot w_z^p(r, z = h^+) &= \\ u_z^l(r, z = h^-) & \\ p^p(r, z = h^+) - p^l(r, z = h^-) &= 0 \\ \sigma_{zz}^p(r, z = h^+) - \sigma_{zz}^l(r, z = h^-) &= 0 \\ \sigma_{zr}^p(r, z = h^+) &= 0 \end{aligned} \quad (24)$$

in which ϕ : is the porosity and w_z^p : is the vertical displacement of pore pressure relative to solid skeleton and has a value of (Pooladi et al., 2017):

$$w_z^p = \frac{\bar{K}_z}{(i\omega)} (\rho_f \omega^2 \bar{\Delta}_z^m - \bar{\Delta}_p^m \frac{d^2}{dz^2}) F \quad (25)$$

To clarify the first relation in Eq. (13), it can be considered that the area of S and the porosity ratio ϕ for the porous medium. By considering a displacement equal to u_z^{liq} in the liquid layer in z direction, the variation of volume in liquid layer will have the value of $S \cdot u_z^{liq}$. According to the principle of continuity the variation of volume in both

layers must have the same values. This value for porous layer is:

$$\begin{aligned}
 S.u_z^{liq} &= S.\varphi.u_z^{pore\ fluid} + \\
 &S.(1 - \varphi)u_z^{solid\ skeleton} \\
 &= S(\varphi u_z^f + u_z^s - \varphi u_z^s) \\
 &= S(u_z^s + \varphi(u_z^f - u_z^s)) \\
 &= S(u_z + \varphi.w_z)
 \end{aligned}
 \tag{26}$$

So, $u_z^{liq} = u_z^p + \varphi.w_z$.

Now the matrix form of the equations can be written as:

$$M(\xi).X(\xi, m) = B(\xi, m) \tag{27}$$

where the elements of matrix M can be easily achieved by using Eqs. (26) and (27).

3. Closed Form

Solving Eq. (13), and finding unknown vector X , will yields the closed form of the Green's functions. If the exciting load be assumed as point source, the excitation source has the function as:

$$f_v(r, \theta, z) = F_v \frac{\delta(r)}{2\pi r} \delta(z - s) e^{i\omega t} \mathbf{e}_z \tag{28}$$

in which F_v : is the magnitude of load and δ : is Dirac-delta function. Eq. (28) has a Hankel transformed state as:

$$Z = F_v / 2\pi \tag{29}$$

Similarly, for a circular patch load with radius a , the load function in the Hankel

transformed shape can be defined as:

$$Z = \frac{F_v J_1(a\xi)}{\pi a \xi} \tag{30}$$

By substitution of the Eq. (28), or (29), into the B vector in the Eq. (27), the closed form has been evaluated. The answers that are obtained here are in Hankel state. By an invert Hankel integral transform, the results in frequency domain will be calculated as:

$$f(r, z; \omega) = \int_0^\infty F(\xi, z; \omega) \xi J_0(r\xi) d\xi \tag{31}$$

The branch points and poles of the integration related to poroelastic materials are complex-valued, so real axis is free from any singularities.

4. Numerical Verification

To show the efficiency of the method that is used here, the solutions are comprised with existing result of some special forms. For comparison, it is assumed that the $h = 0$ and the answers comprised with the existing answers (Pooladi et al., 2017).

In another special state, the half-space is assumed as a solid transversely isotropic material and the answers are compared with available results (Abubakar and Hudson, 1961). The answers show that the phase velocity dispersion of Stoneley wave has a good agreement in both works. The material which were used in this paper have the properties of a Beryl rock as Table 1 (Abubakar and Hudson, 1961).

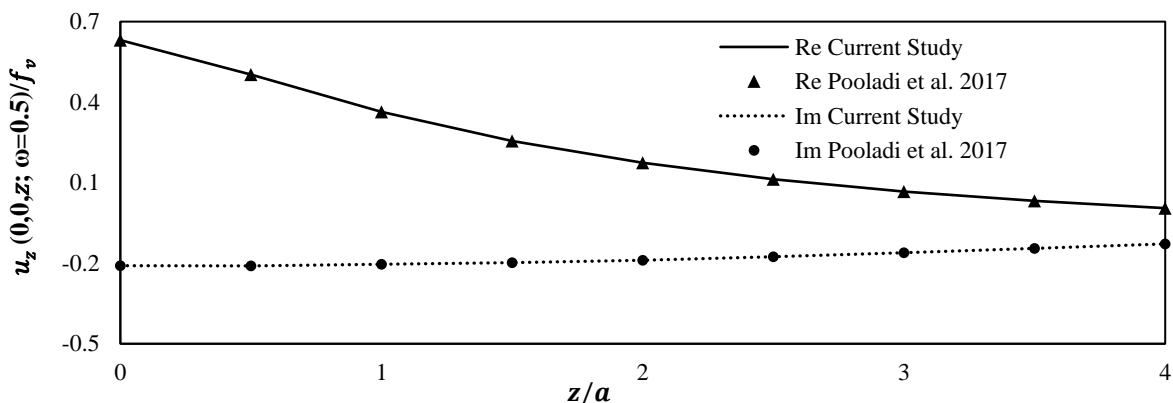


Fig. 3. Real and imaginary parts of u_z for transversely isotropic one layered porous media (Pooladi et al., 2017)

Table 1. Material properties of Solid at (Abubakar and Hudson, 1961)

ρ_s/ρ_l	c_{sv}/c_l	c_p/c_{sv}
2	1.414	2.032

In this table, C_{sv} and C_p : are respectively the velocity of SV and P waves in the bed rock. Also C_l : is the compressional wave velocity in the liquid. It should be noted that the horizontal axis is normalized by multiplying the wave number ξ at the depth of the liquid h . The equation of dispersion of wave velocity is calculated by equating the determinant of matrix **M**.

5. Numerical Results

To study the effect of anisotropy, frequency, and the depth of the liquid layer,

the numerical results have been obtained for different values of these parameters. The basic material properties used in this section are similar to Table 2. The constants in Tables 1 and 2 are for isotropic materials. To illustrate the effect of anisotropy values for ne are used, which is the ratio of E'/E . Where E' and E denote Young's moduli in the plane of isotropy and in the direction normal to it (along the z -axis). Source of excitation is assumed as a circle area with radius of a , and at the interface of two layers. In Figures 5-8, the numerical result for $h=a$ are represented for two different frequencies. The horizontal axis of displacements is normalized by $u^* = u/f_v$ and the vertical axis by z/a .

Table 2. The non-dimensional material properties of porous media (Pooladi et al., 2017)

Material	A_{11}	A_{12}	A_{33}	A_{13}	A_{44}	M	ρ	ρ_f	b	β	m	ϕ
Mat 1	3.5	1.5	3.5	1.5	1	12.2	1	0.53	10	0.97	1.10	0.4

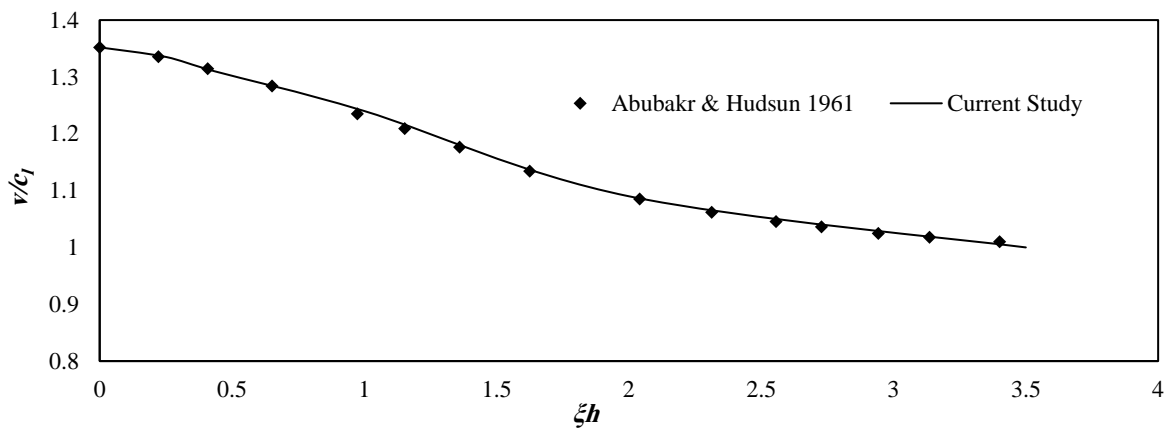


Fig. 4. Stoneley wave phase velocity for a liquid overlying on a transversely isotropic bed rock (Abubakar and Hudson, 1961)

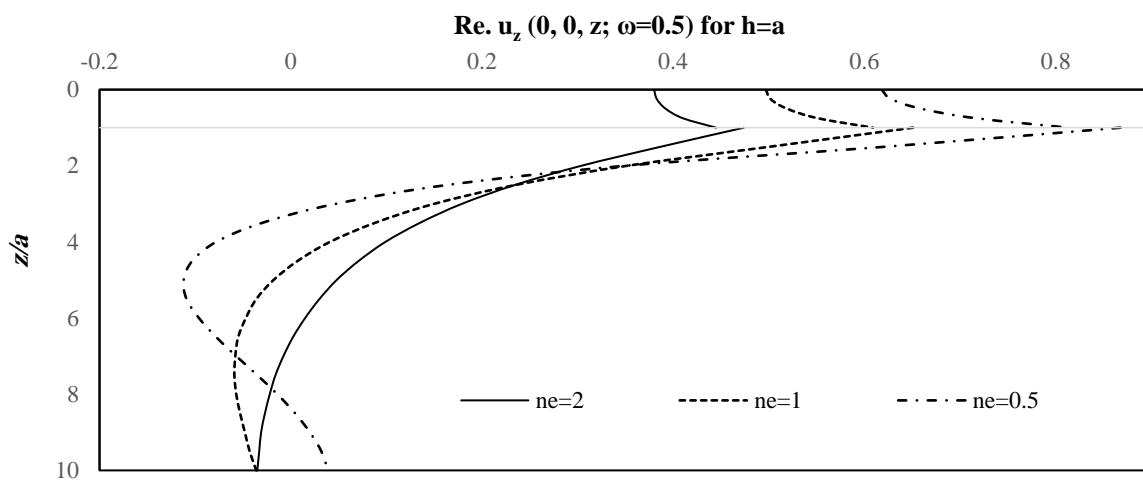


Fig. 5. Real parts of patch-load displacement Green's functions u_z along z axis for $\omega = 0.5$

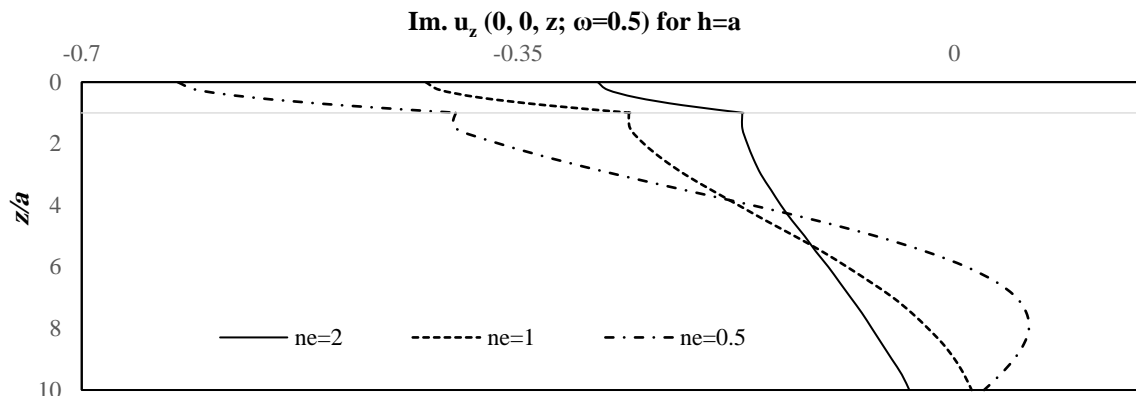


Fig. 6. Imaginary parts of patch-load displacement Green's functions u_z along z axis for $\omega = 0.5$

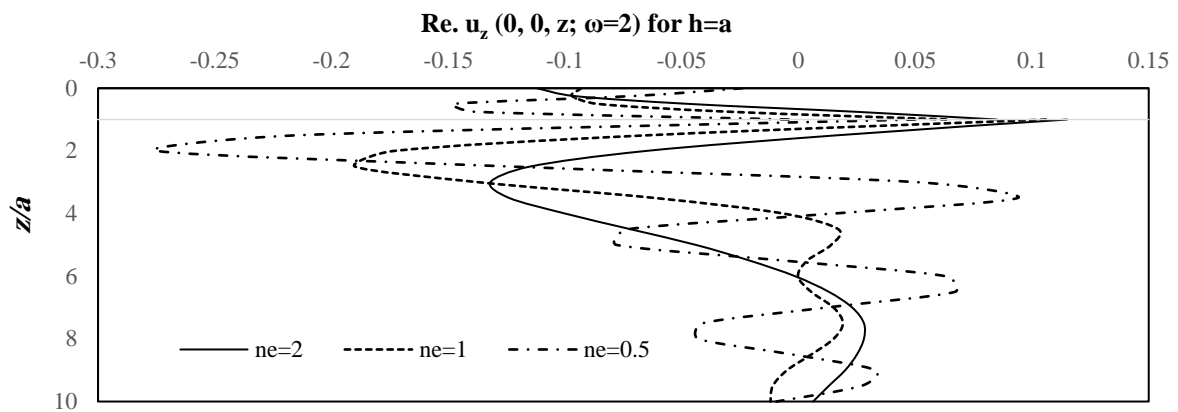


Fig. 7. Real parts of patch-load displacement Green's functions u_z along z axis for $\omega = 2$

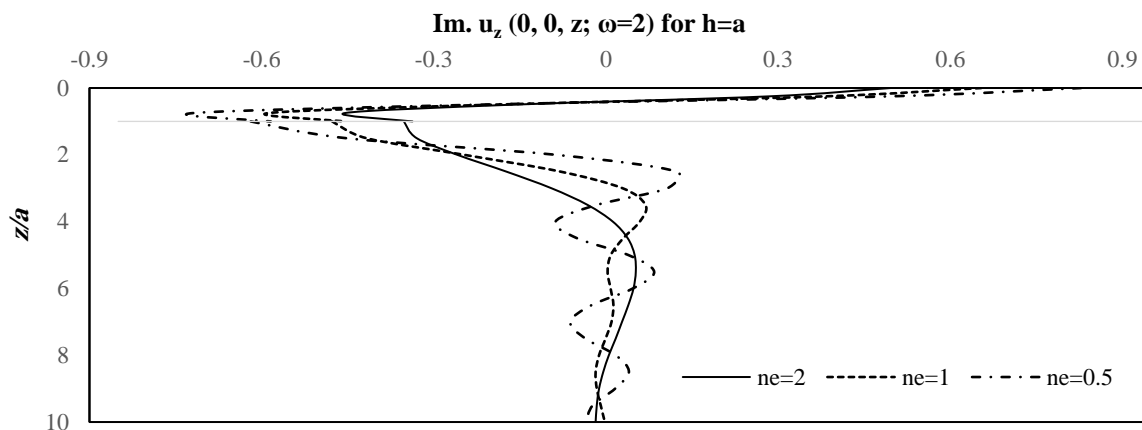


Fig. 8. Imaginary parts of patch-load displacement Green's functions u_z along z axis for $\omega = 2$

As it is clear in the profiles, the vertical displacement increases with the reduction in the value of ne , which generally reflect the effect of Young's moduli in vertical direction normal to the plane of isotropy. Also when the frequency or ne increases, the oscillation behavior of the medium has been increased.

Figures 9 and 10, show the stresses in the media with two different liquid layer thicknesses. As the profiles exhibit, with

reduction in the liquid thickness, the real part of the normal stresses in the porous half-space, at the interface increases and the oscillation behavior of the liquid layer decreases. However, the oscillation behavior in porous half-spaces in both thicknesses are similar.

6. Discussion and Conclusions

In the present paper an analytical treatment

exhibited to solve the elastodynamic boundary value problems concerning a liquid layer with limited thickness, overlying on a transversely isotropic poroelastic half-space. The exciting load was assumed to be at the interface of two media, and with axisymmetric shape. Potential function method has been used to solve the differential equations, and stresses and displacements in two media, has been expressed in terms of potential function. A computer code were developed to evaluate the integrals to obtain results of interior displacements and stresses.

From the results it is obvious that the liquid layer thickness has an important role in the results. As the figures show, the magnitude of stress in each domain depends on the liquid thickness. Also by increasing the liquid layer thickness, the displacement

at the interface will increase.

Anisotropy degree is another important parameter that affect the results. Numerical results demonstrate that, when the deformability in of the half-space material in the direction parallel to the load decreases, the oscillatory behavior in displacements (both real and imaginary parts) have noticeable reduction. The frequency has a key role in results too, its effect is similar to anisotropy degrees. As the frequency increases, of the results show more oscillatory behavior. In high frequencies, resultant disturbances decrease in amplitude at points far from the excitation. In low frequencies the maximum value of the results occurs at the load level. However, in high frequencies it may occur in both mediums, and it depends on the anisotropy degree.

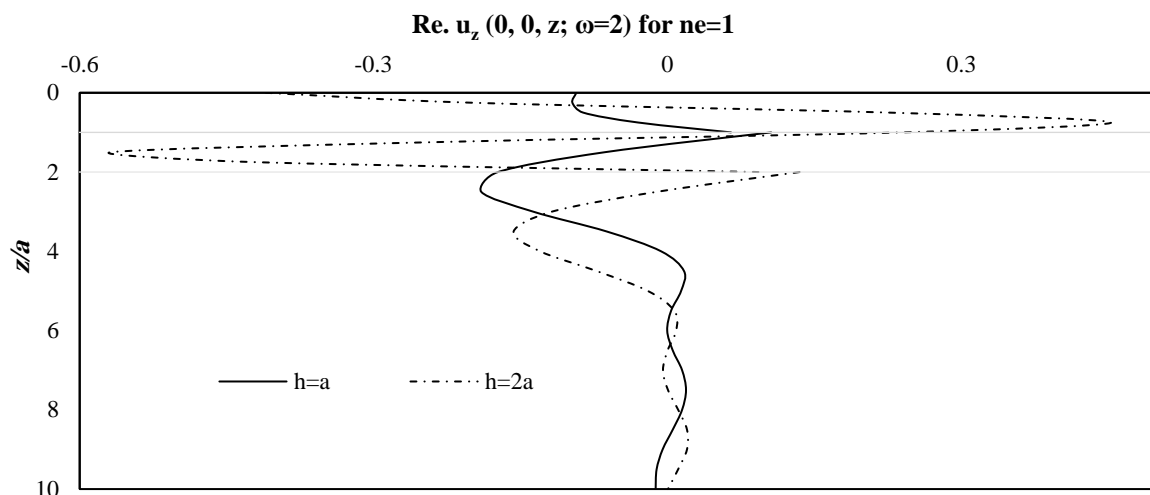


Fig. 9. Real parts of patch-load stresses Green's functions u_z along z axis for $\omega = 2$

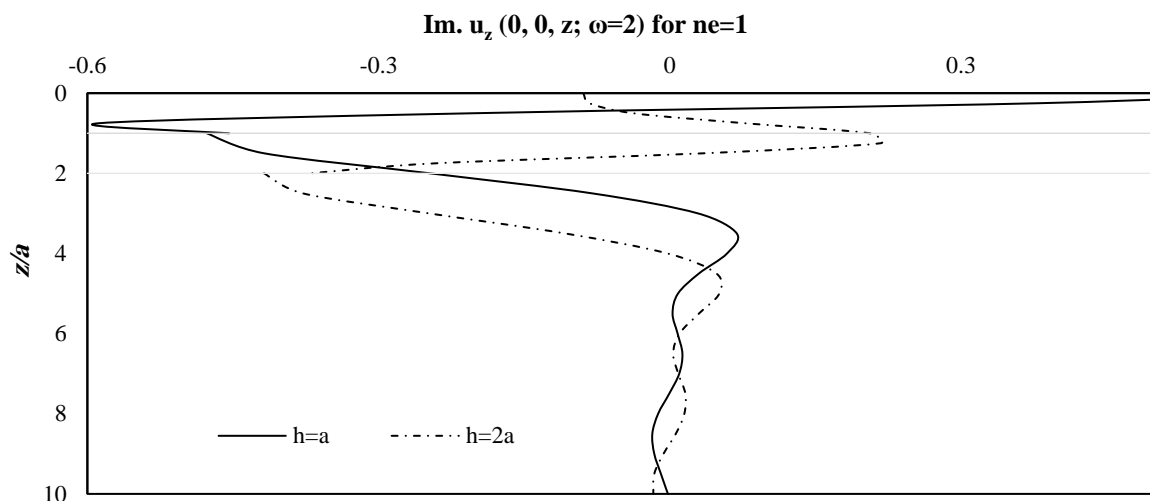


Fig. 10. Imaginary parts of patch-load stresses Green's functions u_z along z axis for $\omega = 2$

In all the figures, (except real part of stresses) there is a gradient discontinuity in plane that load acts. But in stress profiles, the real parts undergo a jump but the imaginary part remain continues.

6. References

- Abubakar, I. and Hudson, J.A. (1961). "Dispersive properties of liquid overlying an aelotropic half-space", *Geophysical Journal International*, 5(3), 217-229.
- Ahmadi, S.F. and Eskandari, M. (2014). "Rocking rotation of a rigid disk embedded in a transversely isotropic half-Space", *Civil Engineering Infrastructures Journal*, 47(1), 125-138.
- Bagheri, A., Khojasteh, A., Rahimian, M. and Greenhalgh, S. (2016). "Dynamic Green's functions for a liquid layer overlying a transversely isotropic solid half-space due to an arbitrary source excitation within the liquid", *Wave Motion*, 63, 83-97.
- Biot, M.A. (1956a). "The theory of propagation of elastic waves in a fluid-saturated porous solid I, Low- frequency range", *The Journal of the Acoustical Society of America*, 28(2), 168-178.
- Biot, M.A. (1956b). "The theory of propagation of elastic waves in a fluid-saturated porous solid, II: Higher frequency range", *The Journal of the Acoustical Society of America*, 28(2), 179-191.
- Cheng, A.H.D. (2016). *Poroelasticity*, Springer, Mississippi.
- Cheng, A.H.D. (1997). "Material coefficients of anisotropic poroelasticity", *International Journal of Rock Mechanics and Mining Sciences*, 34(2), 199-205.
- Eskandari-Ghadi, M.A. (2005). "Complete solution of the wave equations for transversely isotropic media", *Journal of Elasticity*, 81(1), 1-19.
- Feng, S.J., Chen, Z.L. and Chen, H.X. (2016). "Reflection and transmission of plane waves at an interface of water/multilayered porous sediment overlying solid substrate", *Ocean Engineering*, 126, 217-231.
- Keawsawasvong, S. and Senjuntichai. T. (2018). "Influence of anisotropic properties on vertical vibrations of circular foundation on saturated elastic layer", *Mechanics Research Communications*, 94, 102-109.
- Keawsawasvong, S. and Senjuntichai. T. (2019). "Poroelastodynamic fundamental solutions of transversely isotropic half-plane", *Computers and Geotechnics*, 106, 52-67.
- Lian-Zhou, X., Zhang, J., Lv, H.J., Chen, J.J. and Wang. J. (2017). "Numerical analysis on random wave-induced porous seabed response", *Marine Georesource and Geotechnology*, 36(8), 974-985.
- Pooladi, A., Rahimian, M. and Pak, R.J. (2017). "Poroelastodynamic potential method for transversely isotropic fluid-saturated poroelastic media", *Applied Mathematical Modelling*, 50, 177-199.
- Raoofian Naeeni, M. and Eskandari-Ghadi, M. (2014). "A potential method for body and surface wave propagation in transversely isotropic half- and full-spaces", *Civil Engineering Infrastructures Journal*, 49(2), 263-288.
- Sahebkar, K. and Eskandari-Ghadi, M. (2016). "Time-harmonic response of saturated porous transversely isotropic half-space under surface tractions", *Journal of Hydrology*, 537, 61-73.
- Senjuntichai, T. and Rajapakse, R.K.N.D. (1994). "Dynamic Green's functions of homogeneous poroelastic half-space", *Journal of Engineering Mechanics, ASCE*, 120(11), 2381-2404.
- Sharma, M.D. and Gogna, M.L. (1991). "Wave propagation in anisotropic liquid-saturated porous solids", *The Journal of the Acoustical Society of America*, 90(2), 1068-1073.
- Sharma, M.D. (2008). "Propagation of harmonic plane waves in a general anisotropic porous solid", *Geophysical Journal International*, 172(3), 982-994.
- Tajuddin, M. and Hussaini, S.J. (2005). "Reflection of plane waves at boundaries of a liquid filled poroelastic half-space", *Journal of applied geophysics*, 58(1), 59-86.
- Teymouri, H., Khojasteh, A., Rahimian, M. and Pak, R.Y.S. (2019). "Wave propagation in a transversely isotropic porous ocean bottom", *Marine Georesource and Geotechnology*, 38(6), 923-938.
- Yamamoto, T. (2008). "On the response of a Coulomb-damped poroelastic bed to water waves", *Marine Georesource and Geotechnology*, 5(2), 93-130.



This article is an open-access article distributed under the terms and conditions of the Creative Commons Attribution (CC-BY) license.